DALTON
FULL PAPER

Macrocyclic ligand design. X-Ray, DFT and solution studies of the effect of *N*-methylation and *N*-benzylation of 1,4,10,13-tetraoxa-7,16-diazacyclooctadecane on its affinity for selected transition and post-transition metal ions

Trevor W. Hambley, Leonard F. Lindoy,* Jeffrey R. Reimers, Peter Turner, Gang Wei and Asaph N. Widmer-Cooper

Centre for Heavy Metals Research, School of Chemistry, University of Sydney, NSW 2006, Australia

Received 1st November 2000, Accepted 8th January 2001
First published as an Advance Article on the web 9th February 2001

Potentiometric titration in 95% methanol ($I = 0.1$ mol dm^{-3}, Et_4NClO_4) has been employed to investigate the effect of *N*-methylation and *N*-benzylation of 1,4,10,13-tetraoxa-7,16-diazacyclooctadecane **1** on the binding of all three rings to cobalt(II), nickel(II), copper(II), zinc(II), cadmium(II), silver(I) and lead(II). The results show that enhanced selectivity for silver(I) is exhibited by the di-*N*-benzylated derivative **3** while the analogous dimethylated derivative **2** discriminates for both silver(I) and lead(II). The crystal structures of [Ag(**1**)]PF_6, [Ag(**2**)]PF_6, [Ag(**3**)]PF_6 and [Pb(**1**)$(NO_3)_2$] have been determined. In the silver complexes the NH hydrogens of **1** and the *N*-methyl and *N*-benzyl substituents of the dialkylated derivatives **2** and **3** were found to lie on the same side of the mean donor planes of the co-ordinated macrocycles ('*cis*' arrangements). Density functional theory has been employed to model the silver complexes in both their energy-minimised '*cis*' and '*trans*' configurations. In accordance with the X-ray evidence, the calculations predict that the '*cis*' arrangement is the more stable in each case. The crystal structure of the lead complex of **1** shows a '*trans*' arrangement of its NH groups.

Introduction

Macrocyclic ligands have long been employed for studies involving metal ion recognition.[1] In a recent study the effect of *N*-methylation and *N*-benzylation of a 17-membered N_3O_2-donor macrocyclic ring was demonstrated to yield increased discrimination for silver(I) over nickel(II), cobalt(II), zinc(II), cadmium(II) and lead(II).[2] For example, in the case of the dibenzylated derivative, the binding constant for silver(I) was found to be little affected (it increased slightly) relative to the parent (unsubstituted) ligand complex; in contrast, the constants for the other metal ion complexes all decreased significantly. The origin of the increased selectivity for silver is not well understood, even though it has been known for some time that tertiary amine nitrogens sometimes bind more strongly to silver(I) than do secondary amine nitrogens (the relative binding strengths can be solvent dependent).[3]

Other workers have investigated the effects of *N*-alkylation on the metal binding properties of both open chain and cyclic ligands.[4,5] In general, *N*-alkylation of an amine-containing ligand has been found to result in a drop in stability of its metal complexes relative to the corresponding complexes of the analogous unsubstituted system. However, as in the case of silver(I) mentioned above, such an outcome is not universal. For example, *N*-alkylation of particular chelate ligands has also been shown to lead to an increase in the binding constant for lead(II).[6] It has also been suggested, based on studies involving cyclam and related derivatives, that *N*-alkylation might generally promote enhanced stabilisation of metals in their low oxidation states and, in particular, copper(I) relative to copper(II).[7] If so, this may also provide a rationale for the enhanced stability of *N*-amine ligands towards silver(I). While a number of explanations have been put forward for the above observations associated with *N*-alkylation,[3,6,8,9] it is generally not clear which factor(s) will dominate in a given situation[8] or how widespread the phenomenon is when the systems incorporate a range of mixed donor sites and/or ligand backbone structures.

In the present study, potentiometric titration, X-ray structural and DFT studies of the metal ion binding properties of macrocycles **1**–**3** have been carried out in an attempt to probe structure/function relationships underlying the metal-binding behaviour of these ligand systems.

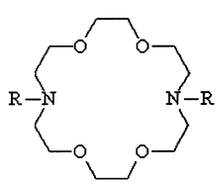

1, R = H

2, R = Me

3, R = benzyl

Experimental

Physical measurements

^{1}H NMR spectra were determined on a Bruker AC200 spectrometer at 200 MHz, in (D)chloroform solution at 25 °C, positive-ion electrospray mass spectra with a Finigan LCQMS Detector (Electrospray Ionisation) spectrometer (samples in methanol or methanol–water).

The stability constants were determined by potentiometric titration. All reagents were analytical grade, with analytical grade methanol being fractionated and distilled over magnesium before use. The apparatus consisted of a water-jacketed measuring cell containing a Philips glass electrode (GA-110) and a water-jacketed calomel reference electrode connected by a salt bridge. A solution of base (tetraethylammonium

 DOI: 10.1039/b008789k

hydroxide) was introduced into the measuring cell by means of a Metrohm dosimat 665 automatic titrator under personal-computer control.

The protonation constants for compounds **1**, **2** and **3** and the corresponding metal stability constants were obtained in 95% methanol ($I = 0.1$ mol dm^{-3}, Et_4NClO_4), with the data processed using a local version of MINIQUAD.[10] The titration data for metal complexation were successfully refined assuming the presence of only 1:1 metal–ligand species in solution; in virtually all cases only data corresponding to the lower portions of the titration curves were employed for the calculations in order to avoid complications arising from competing hydrolysis/precipitation at higher pH values. Quoted log K values (see Table 2) are the mean of between two and five separate determinations obtained at different metal-to-ligand ratios (in each case measured on duplicate sets of the potentiometric titration apparatus).

Structure determination

[Pb(1)][NO$_3$]$_2$. $C_{12}H_{26}N_4O_{10}Pb$, M 593.56, monoclinic, space group $P2_1/c$ (no. 14), a 8.2659(4), b 12.2862(2), c 10.6536(5) Å, $\beta = 110.668(1)°$, V 1012.31(8) Å^3, Z 2, colourless plate, λ(Mo-Kα) 0.71073 Å, μ(Mo-Kα) 84.31 cm^{-1}, N 10860, N_{ind} 2561(R_{merge} 0.0273), N_{obs} 1640($I > 2.5\sigma(I)$), N_{var} 134, $R(F)$ 0.021, $R_w(F)$ 0.022.

[Ag(1)]PF$_6$. $C_{12}H_{26}AgF_6N_2O_4P$, M 515.18, monoclinic, space group $C2/c$ (no. 15), a 15.3255(5), b 8.5474(3), c 14.5016(5) Å, $\beta = 97.427(1)°$, V 1883.7(1) Å^3, Z 4, colourless plate, λ(Mo-Kα) 0.71073 Å, μ(Mo-Kα) 13.63 cm^{-1}, N 9764, N_{ind} 2356(R_{merge} 0.0222), N_{obs} 2027($I > 2.5\sigma(I)$), N_{var} 120, $R(F)$ 0.035, $R_w(F)$ 0.038.

[Ag(2)]PF$_6$. $C_{14}H_{30}AgF_6N_2O_4P$, M 543.23, monoclinic, space group $P2_1/c$ (no. 14), a 14.258(2), b 12.203(1), c 12.622(1) Å, $\beta = 98.895(2)°$, V 2169.7(4) Å^3, Z 4, colourless prism, λ(Mo-Kα) 0.71073 Å, μ(Mo-Kα) 10.72 cm^{-1}, N 22958, N_{ind} 5337(R_{merge} 0.0222), N_{obs} 3333($I > 2.5\sigma(I)$), N_{var} 289, $R(F)$ 0.032, $R_w(F)$ 0.026.

[Ag(3)]PF$_6$. $C_{26}H_{38}AgF_6N_2O_4P$, M 695.42, orthorhombic, space group $Pna2_1$ (no. 33), a 10.6622(6), b 29.681(2), c 9.2715(5) Å, V 2934.1(3) Å^3, Z 4, colourless irregular plate, λ(Mo-Kα) 0.71073 Å, μ(Mo-Kα) 8.14 cm^{-1}, N 31014, N_{ind} 6969(R_{merge} 0.0206), N_{obs} 6345($I > 2\sigma(I)$), N_{var} 369, $R1(F)$ 0.0319, $wR2(F^2)$ 0.0834.

Data collection, structure solution and refinement. Crystals were attached to thin glass fibres and mounted on a Bruker SMART 1000 CCD diffractometer employing graphite monochromated Mo-Kα radiation generated from a sealed tube. Cell constants were obtained from a least square refinement for reflections in the range $2\theta = 4$–56°. Data were collected at 297(2) K with ω scans. In all cases the intensities of a large number of reflections recollected at the end of the experiment did not change significantly during the data collection. Empirical absorption corrections determined with SADABS[11] were applied to the data, and the data integration and reduction were undertaken with SAINT and XPREP.[12] The structures of [Pb(**1**)][NO$_3$]$_2$, [Ag(**1**)]PF$_6$, and [Ag(**2**)]PF$_6$ were solved by direct methods with SHELXS 86,[13] and extended and refined with TEXSAN.[14] Both the complex and counter ion of [Ag(**1**)]PF$_6$ reside on a twofold axis. The counter ion of [Ag(**2**)]PF$_6$ is rotationally disordered about the F(5)–P–F(6) axis. The metal ion of [Pb(**1**)][NO$_3$]$_2$ is located on an inversion centre, and the coordinated nitrate ion exhibits orientational disorder with occupancies of 0.5 assigned to the O(5) and O(6) sites. The structure of [Ag(**3**)]PF$_6$ was solved in the non-centrosymmetric space group $Pna2_1$ (no. 33) by direct methods with SIR 97,[15] and extended and refined with SHELXL 97[16] using the TEXSAN interface.[14] Two residual peaks in the final difference maps were modelled as minor occupancy silver sites, with the populations for Ag(1), Ag(2) and Ag(3) refining to 0.90, 0.04 and 0.06. The minor occupancy silver sites were modelled with isotropic thermal parameters, and the remaining non-hydrogen atoms with anisotropic thermal parameters. A riding atom model was used for the hydrogen atoms. The absolute structure of [Ag(**3**)]PF$_6$ was established with the Flack parameter[17] refining to −0.01(2). ORTEP[18] depictions of the molecules are provided in Figs. 1–4, with ellipsoids shown at the 20 or 30% level.

Selected bond distances and angles for the respective structures are in Table 1.

CCDC reference numbers 152070–152073.

See http://www.rsc.org/suppdata/dt/b0/b008789k/ for crystallographic data in CIF or other electronic format.

DFT Calculations

DFT calculations were carried out in an attempt to gain insight into the factors influencing the somewhat unexpected '*cis*' configurations (see below) observed for the silver complexes in the crystal structures. All calculations were gas phase and only the complex cations were considered (the anion is unco-ordinated in each solid state silver-containing structure.

Two solid-state configurational types were observed for the silver and lead complexes investigated by X-ray diffraction, reflecting the relative orientations of the R substituents on the respective ligands. Namely, for the silver complexes the NH hydrogens of 1,4,10,13-tetraoxa-7,16-diazacyclooctadecane **1** and the *N*-methyl and *N*-benzyl substituents of the dialkylated derivatives **2** and **3** were found to lie on the same side of the mean donor plane of each co-ordinated macrocycle, '*cis*' (or *syn*) arrangement, while the lead complex of **1** was observed to have a '*trans*' (or *anti*) arrangement of its NH groups.

In the computations for the silver complexes the '*cis*' configurations were optimised starting from the corresponding crystal coordinates. The alternative '*trans*' configurations (with the nitrogen substituents lying on different sides of the co-ordination plane) were refined employing the coordinates from the crystal structure of [Cd(**1**)]I$_2$[19] as the starting point, with the coordinates for the methyl and benzyl groups being contributed manually before refinement. The benzyl groups were added such that they were arranged coplanar with, and pointing away from, the mean plane of the macrocyclic ring.

All calculations were carried out using the TURBOMOLE[20] program package, employing the BP86[21] functional. This functional has previously been shown to give satisfactory geometries for several other silver–macrocycle complexes,[22] as well as for model amine and hydroxy complexes.[23] The present calculations were performed using the additional approximation that the coulomb integrals are approximated by a sum of atom centred s, p, d . . . functions, the auxiliary (or fitting) basis.[24] This allows for efficient treatment of the coulomb interactions, and hence reduces the time for a given calculation.

The SV(P) main,[25] and auxiliary,[26] basis sets were used. The main basis set is of [5s3p2d] quality for Ag, [5s2p1d] for C, N and O, and [2s] for H. In addition, the 28 electron relativistic effective core potential of Andrae *et al.*[27] was used for silver in all calculations. Basis Set Superposition Errors (BSSE)s were calculated using the Counterpoise method.[28] BSSE is an undesirable consequence of using finite basis sets that leads to an overestimation of the binding energy.

It needs to be noted that although the BSSEs are of similar magnitude (20–40 kJ mol^{-1}) to the observed differences in complex and binding energies, they are all in the same direction and of approximately equal magnitude. Hence, the errors in relative complex and binding energies due to the BSSE are perhaps only about 20 percent of the calculated BSSE values

(that is, 4–8 kJ mol^{-1}) and the present conclusions concerning relative stabilities are almost certainly valid. Nevertheless, care should be taken when interpreting the relative strain and relative binding energies; the strain energies are the relative energies of the ligands in their geometry found within the '*trans*' and '*cis*' complexes, and therefore include lone-pair interactions, while the binding energies compared are static (energy of complex less that of the silver ion and that of the ligand, with the ligand at the geometry found within the complex), and therefore do not include energy contributions due to changes in ligand geometry.

Ligand syntheses

Macrocycles **1**,[29] **2**[8] and **3**[29] were synthesized using published procedures. The purity of the respective products was confirmed by ^{1}H NMR and microanalysis (Found: C, 54.7; H, 9.9; N, 10.6. $C_6H_{13}NO_2$ **1** requires C, 54.9; H, 10.0; N, 10.7%. Found: C, 57.7; H, 10.1; N, 9.4. $C_7H_{15}NO_2$ **2** requires C, 57.9; H, 10.4; N, 9.7%. Found: C, 70.3; H, 8.4; N, 6.2. $C_{13}H_{19}NO_2$ **3** requires C, 70.6; H, 8.0; N, 6.3%).

Metal complex syntheses

[Ag(1)]PF_6 and [Ag(2)]PF_6. Silver hexafluorophosphate (0.2 mmol) in hot ethanol (10 mL) was added slowly to the respective macrocycle (0.2 mmol) in hot ethanol (10 mL) and the mixture stirred with heating for 30 min. The solution was filtered and allowed to cool to ambient temperature. Colourless crystals of [Ag(**1**)]PF_6 formed and were recrystallised from hot ethanol (Found: C, 27.6; H, 4.6; N, 5.8. $C_{12}H_{26}AgF_6N_2O_4P$ requires C, 28.0; H, 5.1; N, 5.5%). Mass spectrum (ES): *m*/*z* 369.0 ($[AgL]^+$). Colourless crystals of [Ag(**2**)]PF_6 formed after vapour diffusion of diethyl ether into the filtered solution over several days (Found: C, 30.7; H, 5.5; N, 5.5. $C_{14}H_{30}AgF_6N_2O_4P$ requires C, 31.0; H, 5.6; N, 5.2%). Mass spectrum (ES): *m*/*z* 397.0 ($[AgL]^+$).

[Ag(3)]PF_6. Silver nitrate (0.084 g, 0.5 mmol) in hot ethanol (10 mL) was added slowly to compound **3** (0.23 g, 0.5 mmol) in hot ethanol (10 mL) and the mixture heated with stirring for 30 min (**CAUTION**: ethanol solutions of silver nitrate are potentially explosive). The mixture was filtered and allowed to cool to ambient temperature. Tetrabutylammonium hexafluorophosphate (0.19 g, 0.5 mmol) in hot ethanol (5 mL) was added and the mixture stirred for 5 min and allowed to cool to ambient temperature. The colourless crystals formed were filtered off and washed with ethanol (Found: C, 44.9; H, 5.2; N, 4.3; $C_{26}H_{38}AgF_6N_2O_4P$ requires C, 44.9; H, 5.5; N, 4.0%). Mass spectrum (ES): *m*/*z* 549.2 ($[AgL]^+$).

[Pb(1)][NO_3]$_2$·¼EtOH. Lead(II) nitrate (0.2 mmol) in hot ethanol (20 mL) was added slowly to compound **1** (0.2 mmol) in hot ethanol (10 mL) and the solution heated with stirring for 30 min. The solution was filtered and allowed to cool to ambient temperature. Colourless crystals formed after vapour diffusion of ether into the solution over several days (Found: C, 24.8; H, 4.6; N, 9.6. $C_{50}H_{110}N_{16}O_{41}Pb_4$ requires C, 24.8; H, 4.6; N, 9.3%). Mass spectrum (ES): *m*/*z* 234.9 ($[PbL]^{2+}$). The product was recrystallised from hot ethanol to yield crystals suitable for X-ray crystallography.

Results and discussion

X-Ray diffraction study

X-Ray structural analyses of the silver(I) hexafluorophosphate complexes of compounds **1**–**3** (Figs. 1–3) and the lead(II) nitrate complex of **1** (Fig. 4) were undertaken.

The lead complex is effectively ten-co-ordinate (Fig. 4) and, although not unique, this is a high co-ordination number for this metal. Both nitrato ligands co-ordinated to the lead atom in a bidentate fashion. Details of the bond distances and angles

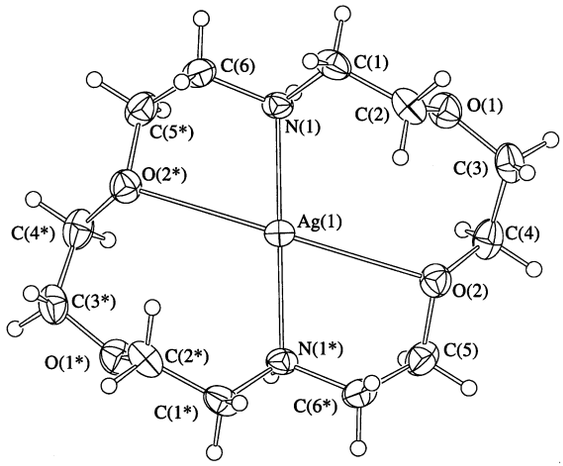

Fig. 1 Crystal structure of [Ag(**1**)]PF_6.

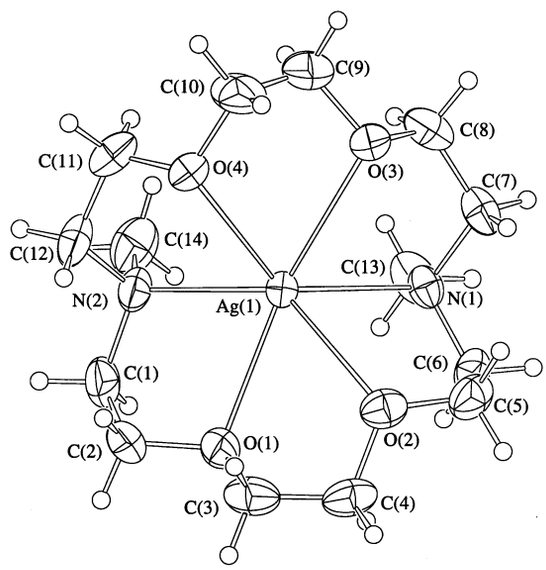

Fig. 2 Crystal structure of [Ag(**2**)]PF_6.

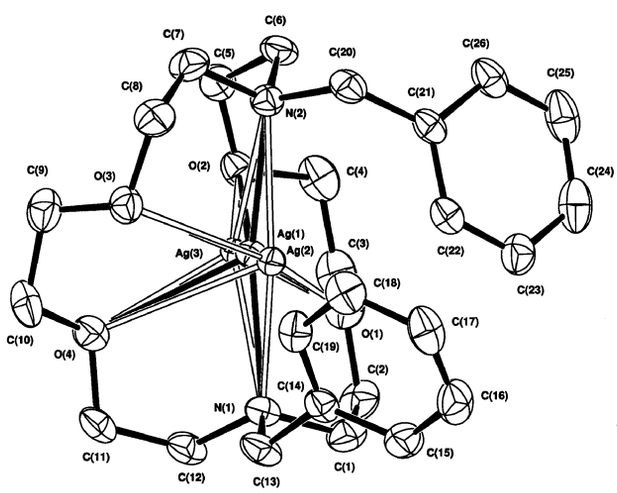

Fig. 3 Crystal structure of [Ag(**3**)]PF_6.

are given in Table 1). As mentioned already, the macrocyclic ligand is arranged in a '*trans*' configuration; the nitrogen hydrogens lie on the same side of the macrocyclic ring. Related '*trans*' arrangements are also observed in the crystal structures of [Cd(**1**)I_2],[19] [Pb(**1**)(SCN)$_2$][30] and [Ni(**1**)Br_2].[31]

In contrast to the above complexes, the anion is non-co-ordinated in each of the present silver(I) complexes and the respective nitrogen substituents are arranged '*cis*' with respect to each other; namely, they are oriented towards the same

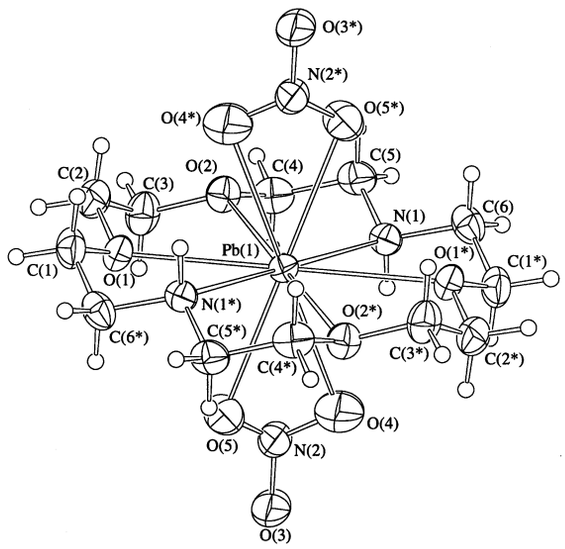

Fig. 4 Crystal structure of $[Pb(\mathbf{1})][NO_3]_2$.

side of each (twisted) macrocyclic ring. The previously reported crystal structure of the potassium complex of the bis-*N*-isopropyl derivative of **1** also shows a similar '*cis*' arrangement of its alkyl substituents.[32] More recently, the structures of two forms of the sodium iodide complex of **3**, namely [Na(**3**)]I and $[Na(\mathbf{3})(H_2O)]I$, have also been reported.[33] In both cases a '*cis*' arrangement is again observed.

The silver ion adopts an almost planar four-co-ordinate arrangement in its complex of **1** (Fig. 1), with two short Ag–N bonds [2.196(2) Å] and two long Ag–O bonds [2.801(2) Å] (Table 1). The N–Ag–N moiety is almost linear [175.8(1)°], consistent with Ag–N bonds being the dominant interactions. The structure contains two non-co-ordinating macrocyclic oxygen atoms (Ag · · · O > 3.5 Å) and both are involved in an intermolecular hydrogen-bonding network that also involves the secondary amine groups; the network extends throughout the crystal such that each macrocycle is associated with four hydrogen bonds.

In $[Ag(\mathbf{2})]PF_6$ (Fig. 2) the macrocycle forms a similar bowl-shaped cavity to that found in the sodium iodide complex of **3**.[33] The silver is six co-ordinate, with the metal lying out of the mean donor plane of the macrocycle and, as mentioned above, the methyl substituents orientated '*cis*'. From initial inspection of CPK (Corey–Pauling–Koltun) models it appeared that the *N*-methyl groups will experience less steric interactions in this arrangement than would occur if a '*trans*' configuration was adopted, a conclusion in keeping with the results of our DFT calculations (see later). The Ag–N and Ag–O bonds are closer in value than in $[Ag(\mathbf{1})]PF_6$ (Table 1).

The '*cis*' complex cation of $[Ag(\mathbf{3})]PF_6$ has all ring nitrogen and oxygen atoms bound to the silver (Fig. 3). An offset T-type π-stacking interaction is present between the phenyl residues, with C(22) lying 3.58 Å above the C(14)–C(19) least squares plane.[34] Such an arrangement corresponds to a pseudo crypt-and being formed around the silver ion. The arrangement adopted is related to that observed in several silver(I) cryptates [namely, those based on **1** with an extra 'strap', incorporating an aromatic ring, connecting the two nitrogen atoms].[8,35] Once again, the metal lies out of the mean donor plane of the macrocycle. While the structure raises the possibility that silver is involved in π interactions with the aromatic rings, the minimum distance between the silver ion and an aromatic ring is about 3.1 Å; this is considerably longer than the 2.5 Å reported for silver(I)–aromatic π bonding in some other systems.[36] It is noted that Ag(2) and Ag(3) correspond to minor occupancy sites in the crystal with populations of 4 and 6%, respectively.

While the Ag–N bond lengths in the *N*-alkylated complexes are longer than the corresponding bonds in the parent complex

Table 1 Bond distances (Å) and angles (°) about the metal atom

(a) $[Ag(\mathbf{1})]PF_6$[a]			
Ag(1)–O(2)	2.801(2)	Ag(1)–N(1)	2.196(2)
O(2)–Ag(1)–N(1)	107.55(8)	O(2)–Ag(1)–N(1)	71.90(8)
O(2)–Ag(1)–O(2)	165.89(6)	N(1)–Ag(1)–N(1)	175.77(8)
(b) $[Ag(\mathbf{2})]PF_6$			
Ag(1)–O(1)	2.564(2)	Ag(1)–O(4)	2.674(2)
Ag(1)–O(2)	2.741(3)	Ag(1)–N(1)	2.323(2)
Ag(1)–O(3)	2.733(3)	Ag(1)–N(2)	2.342(3)
O(1)–Ag(1)–O(2)	63.00(8)	O(2)–Ag(1)–N(2)	134.19(9)
O(1)–Ag(1)–O(3)	153.19(8)	O(3)–Ag(1)–O(4)	62.55(8)
O(1)–Ag(1)–O(4)	111.88(7)	O(3)–Ag(1)–N(1)	70.52(9)
O(1)–Ag(1)–N(1)	112.54(9)	O(3)–Ag(1)–N(2)	124.64(9)
O(1)–Ag(1)–N(2)	72.1(1)	O(4)–Ag(1)–N(1)	132.70(9)
O(2)–Ag(1)–O(3)	94.96(8)	O(4)–Ag(1)–N(2)	71.8(1)
O(2)–Ag(1)–O(4)	116.58(8)	N(1)–Ag(1)–N(2)	138.2(1)
O(2)–Ag(1)–N(1)	71.73(9)		
(c) $[Ag(\mathbf{3})]PF_6$			
Ag(1)–N(2)	2.385(2)	Ag(1)–N(1)	2.392(3)
Ag(1)–O(1)	2.562(3)	Ag(1)–O(2)	2.698(3)
Ag(1)–O(4)	2.712(3)	Ag(1)–O(3)	2.737(4)
N(2)–Ag(1)–N(1)	164.70(11)	O(1)–Ag(1)–O(4)	108.86(10)
N(2)–Ag(1)–O(1)	113.76(15)	O(2)–Ag(1)–O(4)	96.42(9)
N(1)–Ag(1)–O(1)	69.58(10)	N(2)–Ag(1)–O(3)	71.36(14)
N(2)–Ag(1)–O(2)	72.30(14)	N(1)–Ag(1)–O(3)	108.01(11)
N(1)–Ag(1)–O(2)	120.19(11)	O(1)–Ag(1)–O(3)	169.64(10)
O(1)–Ag(1)–O(2)	61.84(11)	O(2)–Ag(1)–O(3)	113.49(7)
N(2)–Ag(1)–O(4)	121.85(10)	O(4)–Ag(1)–O(3)	61.56(10)
N(1)–Ag(1)–O(4)	68.02(9)		
(d) $[Pb(\mathbf{1})][NO_3]_2$			
Pb(1)–O(1)	2.817(3)	Pb(1)–O(5)	2.696(7)
Pb(1)–O(2)	2.815(3)	Pb(1)–O(6)	2.698(9)
Pb(1)–O(4)	2.764(4)	Pb(1)–N(1)	2.760(4)
O(1)–Pb(1)–O(2)	58.67(8)	O(2)–Pb(1)–O(6*)	109.3(2)
O(1)–Pb(1)–O(2*)	121.33(8)	O(2)–Pb(1)–N(1)	61.2(1)
O(1)–Pb(1)–O(4)	110.8(1)	O(2)–Pb(1)–N(1*)	118.8(1)
O(1)–Pb(1)–O(4*)	69.2(1)	O(4)–Pb(1)–O(5)	43.0(2)
O(1)–Pb(1)–O(5)	71.8(2)	O(4)–Pb(1)–O(5*)	137.0(2)
O(1)–Pb(1)–O(5*)	108.2(2)	O(4)–Pb(1)–O(6)	41.1(2)
O(1)–Pb(1)–O(6)	72.0(2)	O(4)–Pb(1)–O(6*)	138.9(2)
O(1)–Pb(1)–O(6*)	108.0(2)	O(4)–Pb(1)–N(1)	70.6(1)
O(1)–Pb(1)–N(1)	118.51(9)	O(4)–Pb(1)–N(1*)	109.4(1)
O(1)–PB(1)–N(1*)	61.49(9)	O(5)–Pb(1)–O(6)	30.7(2)
O(2)–Pb(1)–O(4)	102.1(1)	O(5)–Pb(1)–O(6*)	149.3(2)
O(2)–Pb(1)–O(4*)	77.9(1)	O(5)–Pb(1)–N(1)	104.6(2)
O(2)–Pb(1)–O(5)	96.8(3)	O(5)–Pb(1)–N(1*)	75.4(2)
O(2)–Pb(1)–O(5*)	83.2(3)	O(6)–Pb(1)–N(1)	77.9(3)
O(2)–Pb(1)–O(6)	70.7(2)	O(6)–Pb(1)–N(1*)	102.1(3)

[a] Asterisked atoms generated with $-x$, y, $0.5 - z$. [b] Asterisked atoms generated with $1 - x$, $-y$, $-z$.

(Table 1), it is not possible to say whether this reflects the increase in co-ordination number in the latter complex, or whether it is (in part) a reflection of steric or other effects due to the presence of *N*-alkylation. However, in other studies we have shown computationally that an increase in the Ag–N bond length upon *N*-alkylation also occurs for model amine complexes in the gas phase, suggesting that it is in fact an intrinsic property of such systems.[23] Comparison of the metal–donor bond lengths of the crystal structures of the silver complexes of **1**–**3** with those in the crystal structure of $[Pb(\mathbf{1})(NO_3)_2]$ (see Table 1) indicates that, as expected, the Ag–N bonds are significantly shorter than the Pb–N bonds (perhaps reducing steric hindrance in this latter case).

The '*cis*' arrangement adopted by compound **3** in the above silver complex contrasts with the structure of the metal-free ligand; the structures of both free **3**[33] and its bis(2,4,6-trinitrophenol) solvate[37] have been reported. In both the last cases **3**

Table 2 Ligand protonation constants and metal stability constants for compounds **1**–**3**[a]

Ligand	log K_1	log K_2	log K_{ML}						
			Co^{II}	Ni^{II}	Cu^{II}	Zn^{II}	Cd^{II}	Ag^{I}	Pb^{II}
1	9.40	7.97	<4	<4	7.6	~4.0	7.11	9.79	9.10
	(0.04)	(0.01)			(0.04)		(0.03)	(0.02)	(0.01)
2	9.37	7.64	<4	<4	6.96	<4	5.74	9.15	10.12
	(0.04)	(0.02)			(0.13)		(0.03)	(0.02)	(0.02)
3	8.34	6.69	<4	<4	~5.4	<4	<4	9.62	8.4
	(0.04)	(0.01)						(0.05)	(0.06)

[a] In 95% methanol; $I = 0.1$ mol dm^{-3}, Et_4NClO_4, 25 °C. Standard deviation in parentheses.

Table 3 Geometric comparisons of crystal and calculated gas phase structures[a] for the '*cis*' configuration of the silver(I) complex cations of compounds **1**–**3**

Ligand	Bond lengths/Å			Bond angles/°			Torsion angles/°		
		Max. difference[c]			Max. difference[c]			Max. difference[c]	
	RMS[b] difference	Involving silver	Other bonds	RMS[b] difference	Involving silver	Other angles	RMS[b] difference	Involving silver	Other angles
1	0.02	0.03	0.03	2.1	8.8	2.4	5.3	12.1	10.4
2	0.05	0.11	0.05	2.1	6.1	4.1	4.7	14.9	5.7
3	0.04	0.14	0.06	1.5	4.6	2.5	3.1	7.4	5.7

[a] Only parameters involving non-hydrogen atoms have been compared. The gas phase structures were optimised starting from the crystal coordinates of the complex cation. [b] RMS refers to the root mean square of all differences between corresponding parameter values for the crystal and DFT structures. [c] Refers to the maximum difference between corresponding parameter values, and has been listed separately for parameters involving silver and parameters involving carbon, nitrogen and oxygen only.

has a similar structure, with the benzyl side arms splaying out from the crown in a '*trans*' configuration. The oxygen atoms are oriented in an endodentate fashion that is typical of most crowns while the nitrogen atoms are arranged exodentate in a manner that minimises steric clashes involving the benzyl groups; this latter mode results in the nitrogen lone pairs pointing inwards towards the macrocyclic cavity. Such 'forced' inwards orientation of nitrogen lone pairs, reflecting the presence of *N*-alkylation, has been postulated to be one source of the additional stability observed for particular metal complexes of *N*-substituted aza-crowns over the corresponding parent (unsubstituted) ring complex.[8]

As an aside, it is noted that while there is no direct evidence for either '*cis*' or '*trans*' configurations of such complexes existing in solution, the prospect that these two configurations (and possibly a third) exist in equilibrium is consistent with the conclusions of an ultrasonic and IR relaxation study of the silver(I) complex of compound **1**.[38] From this it was concluded that in acetonitrile and propylene carbonate the main configurations (for timescales longer than 10^{-13} s) were *endo-endo* inclusive complexes with the silver bound to both nitrogen donors. It was also concluded from this study that there were two or three such configurations undergoing 'intramolecular conversions on the microsecond to nanosecond timescale'.

Metal complex stabilities

As mentioned already, *N*-alkylation of an amine ligand usually results in a lowering of the stability of its corresponding complexes, reflecting increased steric hindrance on complex formation.[5] However, the log *K* values for silver(I) complexation have been found in several cases to show only minor change (higher or lower) on *N*-alkylation of the parent ligand. For example, the appending of *N*-decyl, *N*-octyl, *N*-butyl or *N*-benzyl groups to compound **1** has been reported to result in only little change in the respective binding constants for silver(I) in methanol relative to that for **1** itself.[39]

In the present study binding constants for the complexes of cobalt(II), nickel(II), copper(II), zinc(II), cadmium(II), silver(I) and lead(II) with compounds **1**–**3** were determined potentiometrically in 95 percent methanol ($I = 0.1$ mol dm^{-3}; Et_4NClO_4). Protonation constants and log K_{ML} values for the formation of the 1:1 (metal to ligand) complexes are summarised in Table 2; the values listed for **1** and **2** follow generally similar trends to those reported previously for complex formation of these ligands in water.[40]

The log K_{ML} values confirm that the parent N_2O_4-ring macrocycle **1** forms moderately strong complexes with copper(II), cadmium(II), silver(I) and lead(II) relative to those of cobalt(II), nickel(II) and zinc(II) with the highest affinity of **1** being shown for silver(I), while the value for the lead(II) complex is only slightly lower. As expected, the values for cobalt(II), nickel(II) and zinc(II) remain low for the di-*N*-alkylated systems **2** and **3**. *N*-Alkylation clearly affects the relative metal ion affinities of these ligand systems. Inspection of the log *K* values along the complex series confirms that (bis)-*N*-methylation of **1** (to yield **2**) maintains the selectivity of **1** for silver(I) and lead(II), but with the affinity for silver now dropping below that for lead. Interestingly, the lead(II) complex value initially increases for the dimethylated species **2** but then decreases for the complex of the dibenzylated derivative **3**. Indeed, the latter ligand shows quite respectable selectivity for silver(I) over the other six metal ions investigated. That is, relative to the behaviour of **1** and **2**, the affinity of **3** for cadmium(II), copper(II) and lead(II) has been 'detuned', while the log *K* values for silver(I) show only minor variation down the ligand series. It appears likely that a subtle interplay of electronic and structural (including solvational)[3] influences is at work here but, in the absence of further data, it seems inappropriate to speculate on the reason(s) for the behaviour in this case.

Overall, it is clear that the trend noted previously is maintained for the present ligands; namely, that the *N*-benzylation of mixed donor macrocyclic systems initially incorporating secondary amines has only a minor effect on the stabilities of the corresponding silver(I) complexes while the affinity of the ring for other transition and post-transition ions is selectively 'detuned'.

Table 4 Relative energies[a] (kJ mol^{-1}) of calculated '*trans*' and '*cis*' configurations for the silver(I) complex cations of compounds **1**–**3**, and contributing energy terms

Ligand	Relative complex energy[b]	Relative strain energy[c]	Relative binding energy[b,d]	Relative BSSE[e]
1	24	37	13	−0.7
2	22	9	−13	−12.3
3	41	6	−35	−5.7

[a] The relative energy is defined as the difference between the corresponding energy value for the '*trans*' and '*cis*' structures, for example the energy of the '*trans*' complex minus the energy of the '*cis*' complex. Note that the actual values of the complex and ligand energies are negative, so a *positive* relative energy indicates that the '*cis*' complex or ligand is *more stable* than the respective '*trans*' one, while the actual values of the BSSEs and the binding energies are positive, so a *negative* relative energy indicates that the respective BSSE or binding energy is *greater* for the '*cis*' complex. [b] The relative complex and binding energies include corrections for the basis set superposition error (BSSE). [c] The strain energies are the relative energies of the ligands in their geometry found within the '*trans*' and '*cis*' complexes (see[a]). [d] The binding energies compared are static (energy of complex less that of the silver ion and that of the ligand, with the ligand at the geometry found within the complex). [e] BSSE was calculated by the Counterpoise method.[27]

Table 5 Comparison of calculated[a] silver–donor bond lengths in '*cis*' and '*trans*' configurations of the silver(I) complex cations of **1**–**3**

Ligand	Configuration	Ag–N/Å	Ag–O/Å
1	*cis*	2.20	2.82–2.83
	trans	2.35	3.10–3.11
2	*cis*	2.43	3.07
	trans	2.40	3.10–3.11
3	*cis*	2.41–2.42	2.70–2.82
	trans	2.49	3.03–3.05

[a] Details of the '*cis*' structures are as described in the footnote to Table 3. '*trans*' Structures were calculated starting from the crystal geometry of the CdI_2 complex of compound **1**;[19] the anions were removed and the cadmium(II) was replaced with a silver(I) ion. For the complexes of **2** and **3**, coordinates for the respective nitrogen substituents were added manually before optimisation; the phenyl groups were added parallel to the plane of the macrocycle and pointing outward from the centre of the macrocyclic ring.

DFT Studies

Gas phase DFT calculations were undertaken for each of the silver complexes of compounds **1**–**3**. In each case both '*cis*' and '*trans*' configurations were found to correspond to minima in the potential energy surface. For all three silver complexes the geometries of the calculated '*cis*' isomers and crystal structures are quite similar (the results are summarised in Table 3). Only corresponding geometric parameters (bond lengths, bond angles and torsion angles) involving non-hydrogen atoms have been compared. The root mean square (RMS) and maximum differences in parameter values between the crystal and calculated structures are reported. On the other hand the corresponding calculated '*trans*' configurations for all three complexes closely resemble those observed in the crystal structures of the related complexes $[Pb(\mathbf{1})(NO_3)_2]$ (this work), $[Cd(\mathbf{1})]I_2$,[19] $[Pb(\mathbf{1})(SCN)_2]$[30] and $[Ni(\mathbf{1})Br_2]$.[31]

In parallel to the results from the X-ray studies, the '*cis*' configuration for each silver complex was found by DFT to be of lower energy than the corresponding '*trans*' configuration; the relative energies are listed in Table 4.

From an analysis of the contributing energy terms (Table 4) as well as the respective silver–donor bond lengths (Table 5), the greater stability of the '*cis*' complexes appears to reflect the presence of generally shorter and stronger silver–donor bonds (especially to oxygen) in the '*cis*' forms and/or a reduction in strain of the co-ordinated ligand. The latter factor appears to dominate in the '*cis*' complex of compound **1**, perhaps related to the fact that the co-ordination geometry involves only four metal–donor bonds in this case (the '*trans*' complex is six-co-ordinate), while the former appears to be the dominant factor for the complexes of **2** and **3**.

The respective geometries corresponding to the complexes of compound **3** in which the silver occupies minor sites [Ag(1) 90%, Ag(2) 4% and Ag(3) 6%, see Fig. 3] were each the subject of a gas-phase DFT analysis. Interestingly, the results predicted relative stabilities for the individual structures that matched the above occupation percentages. However, the potential significance of this result needs to be discounted somewhat since the model used for the DFT study did not include crystal packing forces; the later might be expected to play a major role in behaviour of this type.

While, overall, the above gas-phase DFT results parallel well the solid-state X-ray results, it is noted that considerable caution is necessary in any attempt to extrapolate them to solution behaviour. The inherent flexibility of the current macrocyclic ligand systems will likely result in a range of conformations (and associated varying solvation patterns) being present in solution. While significant progress towards modelling solution behaviour in other systems has been achieved using the molecular dynamics (MD) technique,[41,42] to the best of our knowledge no reliable MD parameters are available for modelling, in particular, the solution energetics of silver complexes of the present type. Similarly, largely due to computational limitations, no attempt has been made to model solvation effects using DFT in the present study.

Conclusion

The results presented provide an additional example of enhanced selectivity for silver(I) being generated on di-*N*-benzylation of a mixed donor macrocycle. The analogous dimethylated derivative was observed to yield discrimination for both silver(I) and lead(II). X-Ray studies of all three silver complexes showed that each adopts a '*cis*' arrangement in the solid state in which the nitrogen substituents (H, methyl or benzyl) are all orientated to the one side of the mean donor atom plane. For each complex, DFT calculations also predict that the '*cis*' arrangement will be preferred over the corresponding '*trans*' one in the gas phase, even though the latter arrangement would be expected to yield a more symmetrical co-ordination sphere in each case. This preference appears to reflect the presence of shorter and stronger silver–donor bonds (especially to oxygen) in the '*cis*' forms and/or a reduction in strain of the co-ordinated ligand.

Acknowledgements

We thank Drs I. M. Atkinson and K. R. Adam of James Cook University for assistance and the Australian Research Council for support.

References

1 L. F. Lindoy, *The Chemistry of Macrocyclic Ligand Complexes*, Cambridge University Press, Cambridge, 1989.
2 L. F. Lindoy, *Pure Appl. Chem.*, 1997, **69**, 2179.

3 A. S. Craig, R. Kataky, R. C. Matthews, D. Parker, G. Ferguson, A. Lough, H. Adams, N. Bailey and H. Schneider, *J. Chem. Soc., Perkin Trans. 2*, 1990, 1523.
4 R. M. Izatt, K. Pawlak, J. S. Bradshaw and R. L. Bruening, *Chem. Rev.*, 1991, **91**, 1721.
5 R. D. Hancock, *Coord. Chem. Rev.*, 1994, **133**, 39.
6 R. D. Hancock, H. Maumela and A. S. de Sousa, *Coord. Chem. Rev.*, 1996, **148**, 315.
7 G. Golub, H. Cohen, P. Paoletti, A. Bencini, L. Messori, I. Bertini and D. Meyerstein, *J. Am. Chem. Soc.*, 1995, **117**, 8353; G. Golub, H. Cohen, P. Paoletti, A. Bencini and D. Meyerstein, *J. Chem. Soc., Dalton Trans.*, 1996, 2055; G. Golub, I. Zilbermann, H. Cohen and D. Meyerstein, *Supramol. Chem.*, 1996, **6**, 275.
8 V. P. Solov'ev, N. N. Strakhova, V. P. Kazachenko, A. F. Solotnov, V. E. Baulin, O. A. Raevsky, V. Rüdiger, F. Eblinger and H.-J. Schneider, *Eur. J. Org. Chem.*, 1998, 1379.
9 D. Meyerstein, *Coord. Chem. Rev.*, 1999, **185–186**, 141.
10 P. Gans, A. Sabatini and A. Vacca, *Inorg. Chim. Acta*, 1976, **18**, 237.
11 G. M. Sheldrick, SADABS, Empirical absorption correction program for area detector data, University of Göttingen, 1996.
12 SMART, SAINT and XPREP, Area detector control and data integration and reduction software, Bruker Analytical X-Ray Instruments Inc., Madison, WI, 1995.
13 G. M. Sheldrick, SHELXS 86, in *Crystallographic Computing 3*, eds. G. M. Sheldrick, C. Krüger and R. Goddard, Oxford University Press, 1985, pp. 175–189.
14 TEXSAN for Windows, Single Crystal Structure Analysis Software, Molecular Structure Corporation, The Woodlands, TX, 1997–1998.
15 A. Altomare, M. Cascarano, C. Giacovazzo and A. Guagliardi, *J. Appl. Crystallogr.*, 1993, **26**, 343.
16 G. M. Sheldrick, SHELXL 97, Program for crystal structure refinement, University of Göttingen, 1997.
17 H. D. Flack, *Acta Crystallogr., Sect. A*, 1983, **39**, 876; G. Bernardinelli and H. D. Flack, *Acta Crystallogr., Sect. A*, 1985, **41**, 500.
18 C. K. Johnson, ORTEP II, Report ORNL-5138, Oak Ridge National Laboratory, Oak Ridge, TN, 1976; S. R. Hall, D. J. du Boulay and R. Olthof-Hazekamp, Xtal 3.6 System, University of Western Australia, 1999.
19 L.-A. Malmsten, *Acta Crystallogr., Sect. B*, 1979, **35**, 1702.
20 R. Ahlrichs, M. Bär, H.-P. Baron, R. Bauernschmitt, S. Böcker, M. Ehrig, K. Eichkorn, S. Elliot, F. Haasse, M. Häser, H. Horn, C. Huber, U. Huniar, M. Kattannek, C. Kölmel, M. Kollwitz, C. Ochsenfeld, H. Öhm, A. Schäfer, U. Schneider, O. Treutler, M. von Arnim, F. Weigend, P. Weis and H. Weiss, TURBOMOLE, Quantum Chemistry Group, University of Karlsruhe, 1997, Version 4.
21 A. D. Becke, *Phys. Rev.*, 1988, 3098; J. P. Perdew, *Phys. Rev.*, 1986, 8822.
22 T. Rambusch, K. Hollmann-Gloe and K. Gloe, *J. Prakt. Chem.*, 1999, **341**, 202.
23 A. N. Widmer-Cooper, L. F. Lindoy and J. R. Reimers, unpublished work.
24 K. Eichkorn, O. Treutler, H. Öhm, M. Häser and R. Ahlrichs, *Chem. Phys. Lett.*, 1995, 652.
25 A. Schäfer, H. Horn and R. Ahlrichs, *J. Chem. Phys.*, 1992, **97**, 2571.
26 K. Eichkorn, F. Weigend, O. Treutler and R. Ahlrichs, *Theor. Chim. Acta*, 1997, 331.
27 D. Andrae, U. Häussermann, M. Dolg, H. Stoll and H. Preuss, *Theor. Chim. Acta*, 1990, 124.
28 S. F. Boys and F. Bernardi, *Mol. Phys.*, 1970, **19**, 553.
29 V. J. Gatto, S. R. Miller and G. W. Gokel, *Org. Synth.*, 1990, **68**, 227.
30 B. Metz and R. Weiss, *Acta Crystallogr., Sect. B*, 1973, **29**, 1088.
31 L. Kh. Minacheva, N. B. Generalova, I. K. Kireeva, V. G. Sakharova, A. Yu. Tsivadze and M. A. Porai-Koshits, *Zh. Neog. Khim.*, 1993, **38**, 1666.
32 K. V. Damu, H. Maumela, R. D. Hancock, J. C. A. Boeyens and S. M. Dobson, *J. Chem. Soc., Dalton Trans.*, 1991, 2717.
33 K. R. Fewings and P. C. Junk, *Aust. J. Chem.*, 1999, **52**, 1109; E. S. Meadows, S. L. De Wall, L. J. Barbour and G. W. Gokel, *Chem. Commun.*, 1999, 1555.
34 G. Davenport and H. D. Flack, *LSQPL Xtal 3.6 System*, eds. S. R. Hall, D. J. de Boulay and R. Olthof-Hazekamp, University of Western Australia, 1999.
35 F. Belaj, A. Trnoska and E. Nachbaur, *Z. Kristallogr.*, 1997, **212**, 355; H. Adrianatoandro, Y. Barrens, P. Mersau, T. P. Desvergne, F. Fages and H. Bouas-Laurent, *Acta Crystallogr., Sect. B*, 1995, **51**, 293.
36 M. Munakata, L. P. Wu, T. Kuroda-Sowa, M. Maekawa, Y. Suenaga, G. L. Ning and T. Kojima, *J. Am. Chem. Soc.*, 1998, **120**, 8610.
37 M. L. Saleh, A. Salhin, B. Saad, K. Sivakumar and H. K. Fun, *Z. Kristallogr.*, 1997, **212**, 107.
38 P. Firman, L. J. Rodriguez, S. Petrucci and E. M. Eyring, *J. Phys. Chem.*, 1992, **96**, 2376.
39 H.-J. Buschmann, E. Schollmeyer, R. Trültzsch and J. Beger, *Thermochim. Acta*, 1993, **213**, 11.
40 P. Corbaux, B. Spiess, F. Arnaud and M.-J. Schwing, *Polyhedron*, 1985, **4**, 1471.
41 See, for example: A. A. Varnek, G. Wipff, A. S. Glebov and D. Feil, *J. Comput. Chem.*, 1995, **16**, 1; G. Wipff and M. Lauterbach, *Supramol. Chem.*, 1995, **6**, 187; A. Varnek and G. Wipff, *THEOCHEM.*, 1996, **363**, 67; P. Guilbaud and G. Wipff, *New J. Chem.*, 1996, **20**, 631; A. Varnek and G. Wipff, *J. Comput. Chem.*, 1996, **17**, 1520; F. Fraternali and G. Wipff, *J. Phys. Org. Chem.*, 1997, **10**, 292; L. Troxler and G. Wipff, *Anal. Sci.*, 1998, **14**, 43; A. Varnek, G. Wipff, A. Bilyk and J. M. Harrowfield, *J. Chem. Soc., Dalton Trans.*, 1999, 4155; M. Baaden, F. Berny, C. Madic and G. Wipff, *J. Phys. Chem. A*, 2000, **104**, 7659.
42 See, for example: L. X. Dang, *J. Am. Chem. Soc.*, 1995, **117**, 6954; T. M. Chang and L. X. Dang, *J. Phys. Chem. B*, 1997, **101**, 10518; S. J. Cho and P. A. Kollman, *J. Org. Chem.*, 1999, **64**, 5787; E. V. Rybak-Akimova, K. Kuczera, G. S. Jas, Y. Deng and D. H. Busch, *Inorg. Chem.*, 1999, **38**, 3423.